Research Article | Vol. 24, No. 15 | 25 Jul 2016 | OPTICS EXPRESS 16649

Optics EXPRESS

QPSK 3R regenerator using a phase sensitive amplifier

A. PERENTOS,[1,2,4] S. FABBRI,[1,3] M. SOROKINA,[1] I. D. PHILLIPS,[1] S. K. TURITSYN,[1] A. D. ELLIS,[1] AND S. SYGLETOS[1,5]

[1]*Aston Institute of Photonic Technologies, Aston University, Birmingham, UK*
[2]*Now at: Department of Electrical and Computer Engineering, University of Cyprus, Cyprus*
[3]*Department of Physics, University College Cork, Ireland*
[4]*perentos@ucy.ac.cy*
[5]*s.sygletos@aston.ac.uk*

Abstract: A black box phase sensitive amplifier based 3R regeneration scheme is proposed for non-return to zero quadrature phase shift keyed formatted signals. Performance improvements of more than 2 dB are achieved at the presence of input phase distortion.

OCIS codes: (060.1155) All-optical networks; (060.1660) Coherent communications; (070.4340) Non-linear optical signal processing; (190.4380) Four-wave mixing; (190.4410) Non-linear optics, parametric processes.

References and links

1. A. D. Ellis, N. Mac Suibhne, D. Saad, and D. N. Payne,"Communication networks beyond the capacity crunch," Phil. Trans. R. Soc. A **374**(2062), 20150191 (2016).
2. H. J. Thiele, A. D. Ellis, and I. D. Phillips,"Recirculating loop demonstration of 40 Gbit/s all-optical 3R data regeneration using a semiconductor nonlinear interferometer," Electron. Lett. **35**(3), 230–231 (1999).
3. M. A. Sorokina and S. K. Turitsyn, "Regeneration limit of classical Shannon capacity," Nat. Commun. **5**, 3861 (2014).
4. M. A. Sorokina, "Design of multilevel amplitude regenerative system," Opt. Lett. **39**(8), 2499–2502 (2014).
5. L. Li and M. Vasiliev, "All-optical 2R regenerator of 16-QAM signals," Proc. SPIE **9009**, 900908 (2013).
6. T. Roethlingshoefer, G. Onishchukov, B. Schmauss, G. Leuchs, "All-optical simultaneous multilevel amplitude and phase regeneration," IEEE Photon. Technol. Lett. **26**(6), 556–559 (2014).
7. J. Kakande, R. Slavik, F. Parmigiani, A. Bogris, D. Syvridis, L. Gruner-Nielsen, R. Phelan, P. Petropoulos, and D. J. Richardson, "Multilevel quantization of optical phase in a novel coherent parametric mixer architecture," Nat. Photonics **5**(12), 748–752 (2011).
8. S. Sygletos, M. E. McCarthy, S. J. Fabbri, M. A. Sorokina, M. F. C. Stephens, I. D. Phillips, E. Giacoumidis, N. M. Suibhne, P. Harper, N. J. Doran, S. K. Turitsyn, and A. D. Ellis, "Multichannel regeneration of dual quadrature signals," in Proceedings of ECOC 2014, paper We.1.5.4.
9. J. Leuthold, B. Mikkelsen, R. E. Behringer, G. Raybon, C. H. Joyner, and P.-A. Besse, "Novel 3R regenerator based on semiconductor optical amplifier delayed-interference configuration," IEEE Photon. Technol. Lett. **13**(8), 860–862 (2001).
10. Z. Zhu, M. Funabashi, P. Zhong, L. Paraschis, D. L. Harris, and S. J. B. Yoo, "High-performance optical 3R regeneration for scalable fiber transmission system applications," J. Lightwave Technol. **25**(2), 504–511 (2007).
11. A. Bogoni, P. Ghelfi, M. Scaffardi, L. Poti, "All-optical regeneration and demultiplexing for 160 Gb/s transmission systems using a NOLM-based three stage scheme," IEEE J. Select. Top. Quantum Electron. **10**(1), 192–196 (2004).
12. W. A. Pender, T. Widdowson, and A. D. Ellis, "Error free operation of a 40 Gbit/s all optical regenerator," Electron. Lett. **32**(6), 567 (1996).
13. M. Matsumoto, "A fiber-based all-optical 3R regenerator for DPSK signals," IEEE Photon. Technol. Lett. **19**(5), 273–275 (2007).
14. T. Otani, T. Miyazaki, and S. Yamamoto, "40-Gb/s optical 3R regenerator using electroabsorption modulators for optical networks," IEEE J. Lightwave Technol. **20**(2), 195–200 (2002).
15. Z. Zhu, M. Funabashi, P. Zhong, X. Bo, L. Paraschis, and S. J .B. Yoo, "Jitter and amplitude noise accumulations in cascaded all-optical regenerators," IEEE J. Lightwave Technol. **26**(12), 1640–1652 (2008).
16. S. Fabbri, S. Sygletos, A. Perentos, E. Pincemin, K. Sugden, and A. D. Ellis, "Experimental implementation of all-optical interferometric drop, add, and extraction multiplexer for optical superchannels," IEEE J. Lightwave Technol. **33**(7), 1351–1357 (2015).
17. E. Pincemin, M. Song, J. Karaki, O. Zia-Chahabi, T. Guillossou, D. Grot, G. Thouenon, C. Betoule, R. Clavier, A. Poudoulec, M. Van der Keur, Y. Jaouen, R. Le Bidan, T. Le Gall, P. Gravey, M. Morvan, B. Dumas-Feris, M. L.

#260291 http://dx.doi.org/10.1364/OE.24.016649
Journal © 2016 Received 10 Mar 2016; revised 21 Apr 2016; accepted 21 Apr 2016; published 14 Jul 2016

Optics EXPRESS

Moulinard, and G. Froc, "Multi-band OFDM transmission at 100 Gbps with sub-band optical switching," IEEE J. Lightwave Technol. **32**(12), 2202–2219 (2014).
18. S. Sygletos, S. Fabbri, E. Giacoumidis, M. Sorokina, D. Marom, M. Stephens, D. Klonidis, I. Tomkos, and A. Ellis, "Numerical investigation of all-optical add-drop multiplexing for spectrally overlapping OFDM signals," Opt. Express **23**(5), 5888–5897 (2015).
19. P. Ohlen and E. Berglind, "BER caused by jitter and amplitude noise in limiting optoelectronic repeaters with excess bandwidth," IEE Proc. Optoelectron. **145**(3), 147–150 (1998).
20. M. A. Sorokina, S. Sygletos, F. Ferreira, A. Perentos, A. Ellis, and S. Turitsyn, "Advanced 3R regenerator scheme for high spectral efficient signal waveforms," in 15th Proceedings of the Internaltional Conference on Transparent Optical Networks (ICTON 2015).
21. K. Croussore, I. Kim, Y. Han, C. Kim, G. Li, and S. Radic, "Demonstration of phase-regeneration of DPSK signals based on phase-sensitive amplification," Opt. Express **13**(11), 3945–3950 (2005).
22. R. Slavik, F. Parmigiani, J. Kakande, C. Lundstrom, M. Sjodin, P. Andrekson, R. Weerasuriya, S. Sygletos, A. D. Ellis, L. Gruner-Nielsen, D. Jakobsen, S. Herstrom, R. Phelan, J. O'Gorman, A. Bogris, D. Syvridis, S. Dasgupta, P. Petropoulos, and D. Richardson, "All-optical phase and amplitude regenerator for next generation telecommunications systems," Nat. Photonics **4**(10), 690–695 (2010).
23. A. D. Ellis, T. Widdowson, X. Shan, and D. G. Moodie, "Three-node, 40 Gbit/s OTDM network experiment using electro-optic switches," Electron. Lett. **30**(16), 1333–1334 (1994).
24. D. Hillerkuss, M. Winter, M. Teschke, A. Marculescu, J. Li, G. Sigurdsson, K. Worms, S. Ben Ezra, N. Narkiss, W. Freude, and J. Leuthold, "Simple all-optical FFT scheme enabling Tbit/s real-time signal processing," Opt. Express **18**(9), 9324–9340 (2010).
25. S. J. Savory, "Digital coherent optical receivers: algorithms and subsystems," IEEE J. Lightwave Technol. **16**(5), 1164–1179 (2010).
26. R. Rudnick, A. Tolmachev, D. Sinefeld, O. Golani, S. Ben-Ezra, M. Nazarathy. D. Marom, "Sub-banded/single-sub-carrier drop-demux and flexible spectral shaping with a fine resolution photonic processor," in Proceedings of ECOC 2014, PD.4.1.
27. R. Schmogrow, B. Nebendahl, M. Winter, A. Josten, D. Hillerkuss, S. Koenig, J. Meyer, M. Dreschmann, M. Huebner, C. Koos, J. Becker, W. Freude, and J. Leuthold, "Error vector magnitude as a performance measure for advanced modulation formats," IEEE Photon. Technol. Lett. **24**(1), 61–63 (2011).

1. Introduction

As capacity demand in optical communication networks is beginning to exceed the nonlinear Shannon limit [1], mid link regeneration is becoming increasingly important. All-optical regeneration prevents the accumulation of the various impairments in long haul optical transmission systems, without the need for opto-electronic conversion and the associated digital signal processing. Prior to the advent of coherent detection, 3R regenerators had been shown to amplify, retime and reshape on-off keyed signals allowing infinite cascadability [2] but were focused on spectrally inefficient RZ pulses with per channel bit rate being a priority over spectral efficiency. With the recent introduction of highly spectrally efficient signals, characterized by non-return to zero (NRZ) modulation of complex constelations (i.e. m-QAM), the retiming functionality was overlooked and the efforts were focused on advancing only the 2R performance. In this respect, all-optical 2R-regenerator schemes scalable to high constellation order have been theoretically proposed [3–6], and experimental implementations have been achieved for the QPSK format in both single- [7] and multi-wavelength [8] operation.

In future transmission systems, the channels will be densely packed and tight filtering will be required for any in-line channel selection, e.g. to perform all-optical add-drop multiplexing or signal regeneration. Unavoidably, this will give rise to reduced phase margin and timing jitter effects that will accumulate along the 2R line, drastically limiting the system cascadability. This limited cascadability in 2R regenerators remains a significant obstacle for commercial deployment and retiming functionality is necessary in order to cascade all-optical regenerators. However, to comply with current multi-level modulated highly spectral efficient transmission systems, NRZ or even Nyquist pulse shapes have to be considered as the input and be presented at the output of the regenerator. All-optical 3R regenerators have been so far implemented with semiconductor optical amplifiers in conjunction with interferometers [2, 9–11], fibre based configurations [12, 13] and electro-absorption modulators [14]. In these previously reported works,

Optics EXPRESS

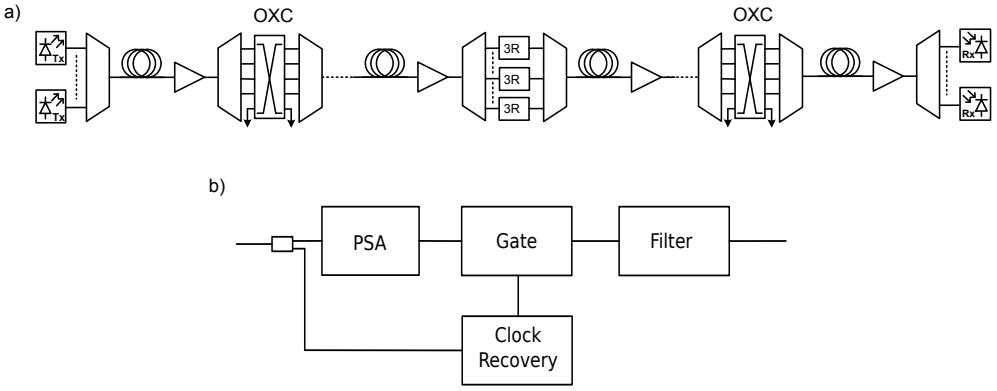

Fig. 1. (a) Schematic of a physical layer transmission path from a typical DWDM network system that employs 3R regenerators and optical cross-connects. (b) Block diagram of proposed 3R regenerator architecture.

spectrally inefficient RZ pulse patterns were mostly used for either OOK or differential phase shift keying (DPSK) modulated signals. A 3R regenerator for NRZ pulses has been reported in [15], but this was also limited to OOK modulation.

In this paper, a phase sensitive amplifier (PSA) based 3R-regenerator for 10.7 Gbaud quadrature phase shift keyed non-return to zero (NRZ-QPSK) signal is demonstrated for the first time. The demonstration is based on a new modular type of 3R architecture that consists of the PSA enabled nonlinear element, followed by an optical gate and a pulse reshaping filter. It is shown that the QPSK signal, degraded by periodic phase modulation at the input of the regenerator can be regenerated in phase, retimed and reshaped back to its original NRZ form for further transmission. Significant improvement in terms of Q^2-factor performance has been achieved. The proposed concept could find application in existing and future dense/ultra-dense wavelength division multiplexed channels including all-optical OFDM and Nyquist WDM where matched demultiplexing filters would need to be added at the regenerator input along with reshaping filters at the output to restore the desired pulse shape [16].

2. Principle of operation

We consider a typical DWDM network system that employs 3R regenerators, see Fig. 1(a). The propagating signals suffer distortions introduced not only by the nonlinear transmission fibre and the inline amplifiers, but also, by the multiplexers/demultiplexers that select and recombine the signals at the regeneration and switching nodes, which is particularly troublesome in optical super channel networks [16, 17]. At the regeneration nodes the degraded signals are demultiplexed and launched to the PSA elements of the 3R subsystems, see Fig. 1(b). Each PSA has the capability of suppressing phase distortions but it is unable to correct timing displacements of the signal waveform at the pulse edges. Subsequently, an optical gate located at the PSA output creates a switching window of finite duration [18] that samples the signal waveform at the areas of minimum inter-symbol interference or crosstalk for optically routed super-channels. The synchronization of the sampling process is achieved by a conventional clock recovery unit that is fed by the same signal waveform that enters the PSA. The sampled signal is then launched to a pulse reformatting filter, with transfer function $H(f) = \mathrm{sinc}(fT)$, which reshapes the pulses back to their initial symbol duration T. Linear optical amplification should be also considered within the regenerator to recover the pulse energy loss associated with the sampling process.

The mechanism of timing jitter accumulation along a 2R cascade has been well described

Optics EXPRESS

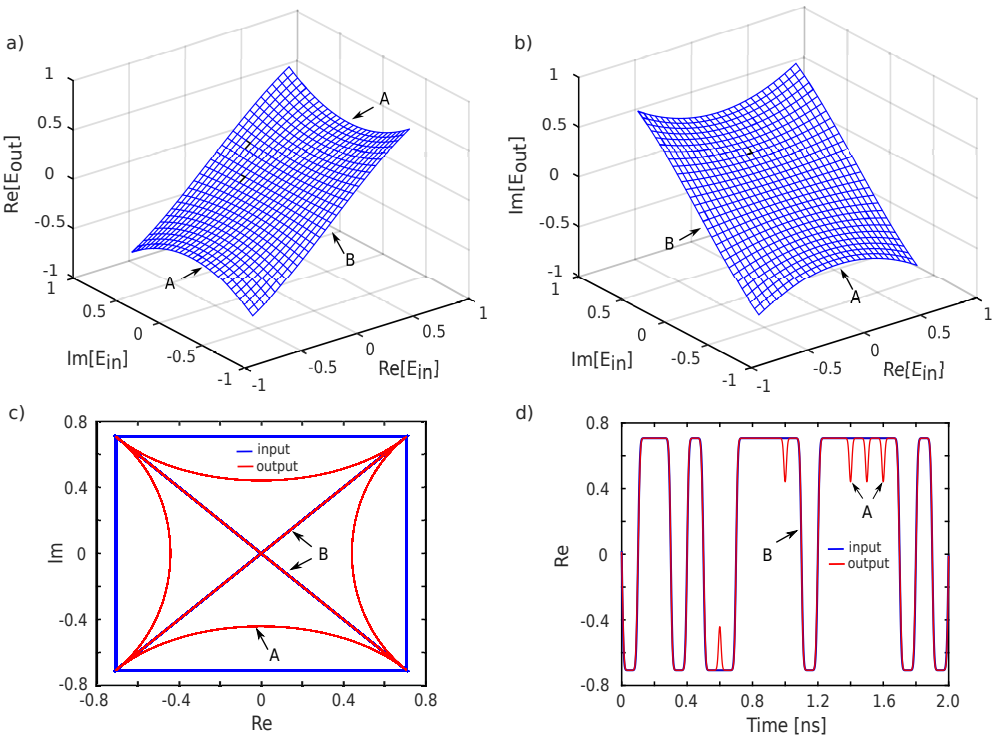

Fig. 2. PSA response in Cartesian coordinates. Specifically, (a) depicts the real part, and (b) the imaginary part of the output signal E_{out}, as a function of the complex coordinates of the input signal E_{in}. The power of the output signal has been normalized with respect to the gain of the PSA. (c) Constellation of QPSK signal at the PSA input (in blue) and corresponding output (in red). Substantial trajectory changes noticed for horizontal or vertical transitions, whereas diagonal transitions remain the same. (d) Corresponding time domain waveforms of real signal quadrature at the PSA input (in blue) and output (in red).

for traditional amplitude shift keying formats [19]. To expand the analysis for QPSK signals it is convenient to consider operation in Cartesian coordinates. Therefore, we assume that the complex signal waveform is generated by independent binary modulation of its real and imaginary parts. Furthermore, the PSA transfer function, which is traditionally expressed in polar coordinates [7], is now mapped in the new coordinate system, see Figs. 2(a) and 2(b). The graphs suggest that simultaneous pulse transitions on the real and imaginary components are transferred linearly to the PSA output, whereas sole transitions give rise to amplitude variations on the respective orthogonal quadrature. This effect is clearly revealed in Figs. 2(c) and 2(d). Specifically, Fig. 2(c) shows the constellation of a 10 Gbaud QPSK waveform at the input of the PSA (in blue), along with the resulting waveform at the output (in red). For the horizontal or vertical transitions, designated by A, a substantial change in the trajectory is noticed, whereas for the diagonal transitions, designated by B, no changes occur. In time domain this means that for each pulse transition on the imaginary component, an “amplitude dip" will appear on the real component of the output signal, see Fig. 2(d), and vice versa. As a result, each PSA will not only leave unsuppressed the distortion on the input pulse edges, known as timing jitter, but it will create additional one and transfer it to the next stage to become further enhanced.

The origin of timing jitter is mainly on the tight filtering of the signal as it propagates through the network nodes. This is a pattern dependent effect, but it acquires a more stochastic nature as

Optics EXPRESS

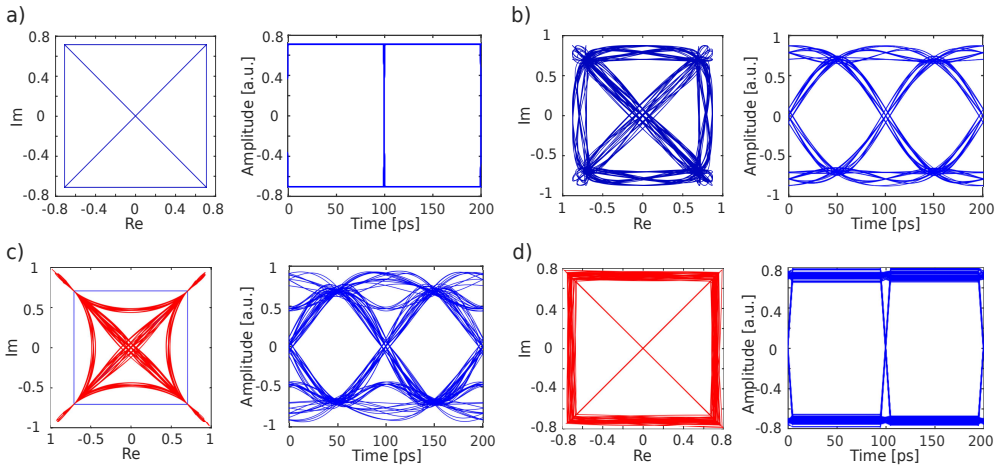

Fig. 3. Constellation and corresponding eye diagrams of the QPSK signal waveform: (a) at the input of the transmission system; (b) at the input of the PSA after strong spectral narrowing accumulated by the transmission process; (c) at the PSA output showing the achieved suppression of the phase distortion at the alphabet points, but also the inability of the PSA to correct the signal waveform during symbol transitions; (d) at the output of the 3R regenerator, demonstrating elimination of the timing uncertainty and recovery of the initial pulse shape.

ASE noise and other noisy-like distortions (e.g. cross-phase modulation) come into play. The capability of the proposed sampling and pulse reshaping scheme to remove timing jitter effects is shown in the constellation and eye diagrams of Figs. 3(a)-3(d). These have been taken assuming a 10 Gbaud QPSK waveform of ideal rectangular pulses at the input of the transmission system, see Fig. 3(a). The total number of simulated symbols was 2048 and the sample-rate was 256 samples per symbol. As the signal propagates through the fibre network it is degraded both in its real and imaginary part. Without loss of generality, we have ignored the influence of fibre non-linearities and ASE noise and we have considered only the degradation by cascaded optical filtering cross wavelength routing devices along the link. The diagrams of Fig. 3(b) depict the signal waveforms at the PSA input after being filtered by an effective 3rd order Gaussian transfer function of 11 GHz full width at half maximum bandwidth. In this example, the predominant effect is that the pulses have lost their rectangular shape by acquiring a long rise-time, however they also suffer from strong data patterning due to I and Q transitions between the same and adjacent pairs of bit slots.

As shown in Fig. 3(c), the PSA suppresses the phase deviations at the alphabet points of the constellation but it does not reduce the timing distortions on the pulse edges, passing them to the next stage. On the other hand, complete removal of the timing jitter is achieved at the re-timing stage of the regenerator based on the proposed sampling and optical filtering processes. A switching window duration of 12 ps was assumed. The diagrams of Fig. 3(d) reveal undistorted, almost pattern effect free, transitions between the pulses and a recovery of their rectangular shape. Some residual amplitude distortion occurs because of the partial, i.e. only on the phase, regeneration the specific PSA configuration can offer to the signal waveform. The use of more advanced regenerator schemes [20] that enable noise suppression on both signal quadratures are expected to eliminate this effect.

There is a fundamental difference in the architecture of the proposed approach compared to most of the 3R regenerator schemes that have been proposed in the past [2,9,10,12–15]. In those

Optics EXPRESS

cases, the re-timing functionality was occurring simultaneously with the noise suppression in the non-linear medium, e.g. the SOA or the HNLF. However, this was imposing a significant degree of complexity in the overall subsystem design, since the non-linear operation of the device had to be adapted to the short time scale of the sampling window. Here the proposed architecture is modular and the two functionalities are decoupled. The PSA regenerator performs only the suppression of the phase noise, whilst the sampling occurs separately by the following gate. In addition, the use of the pulse reshaping filter allows our scheme to operate with spectrally efficient NRZ pulse shapes, contrary to the previous schemes which were limited to RZ pulses. Finally, the freedom that we have in selecting the reshaping filter at the output, highlights the potential of the architecture to operate with different pulse shapes, e.g. Nyquist pulses. However, a detailed investigation of such capability is beyond the scope of this paper.

3. Experimental setup

The experimental setup of the proposed scheme is depicted in Fig. 4. At the transmitter, a 10.7 Gbaud QPSK signal was generated by modulating a 5 kHz linewidth continuous wave (cw) optical beam at 1552.78 nm with a Mach-Zehnder IQ modulator. The modulator was driven by two de-correlated pseudo-random binary sequence (PRBS) data streams of $2^{15}-1$ pattern length. A subsequent phase modulator was used to introduce a 7 GHz sinusoidal phase distortion in the same way as demonstrated in [21, 22], followed by an optical amplifier which raised the signal power to 9.5 dBm. At the input of the regenerator a portion of the optical signal was tapped to a local clock recovery unit and the remaining was directed to a nonlinear stage for the phase synchronization.

The synchronization of the PSA was based on the carrier extraction scheme proposed in [7]. The input QPSK signal was combined with a free running local cw-pump at 1553.91 nm (i.e. Pump-1) and after being amplified to 33 dBm the two signals were launched into a first highly nonlinear fiber (HNLF-1) where a strong four wave mixing (FWM) process gave rise to 3rd and 4th order harmonic products at 1550.54 nm and 1549.42 nm, respectively. The HNLF-1 was a 350 m strained aluminous-silicate spool with a nonlinear coefficient of 7W $^{-}$1 km $^{-}$1 and a dispersion parameter varying in the range of -2 to 2 ps/(nm km). The spool was also characterized by a high stimulated Brillouin threshold ($>$ 35 dBm) and a total loss of 4 dB. The 4th order harmonic was stripped of the data modulation and it was independently self-locked to the combined phase of the QPSK signal and the common pump. Along with the 3rd order harmonic, they maintained a well defined relationship for phase noise squeezing in the subsequent PSA stage. To achieve this, the extracted carrier was selected and used to phase lock a discrete mode laser (DML) through optical injection locking, see lower interferometer path in Fig. 4. The emitted power of the DML was 8 dBm, whereas the injected power was kept below -20 dBm to adequately suppress any residual phase or amplitude distortion of the modulation stripping process. In the upper path of the interferometer the entire FWM spectrum was directed to a wavelength selective switch (WSS), which suppressed all the unwanted spectral components selecting only the waves that were needed for the phase quantization stage, i.e. the free running local pump (Pump-1), the QPSK signal, the 3rd order harmonic and the phase locked pump (Pump-2) of the lower arm.

At the WSS output, the entire shaped spectrum was then amplified by a 30 dBm EDFA and launched to a second nearly identical highly nonlinear fiber (HNLF-2) where the phase sensitive interaction took place. Due to slow temperature-induced path length variations between the interferometric arms of the PSA, phase drifts were present in the setup. These drifts were compensated using an electrical feedback stabilization circuit setup that made use of the 3rd order signal harmonic at the output of the PSA as an error signal to control a piezoelectric fiber stretcher (PZT). The phase squeezed signal was then fed to an optical gate in order to sample the data at the optimum point and thus to implement the retiming operation. The gate [23] comprised

Optics EXPRESS

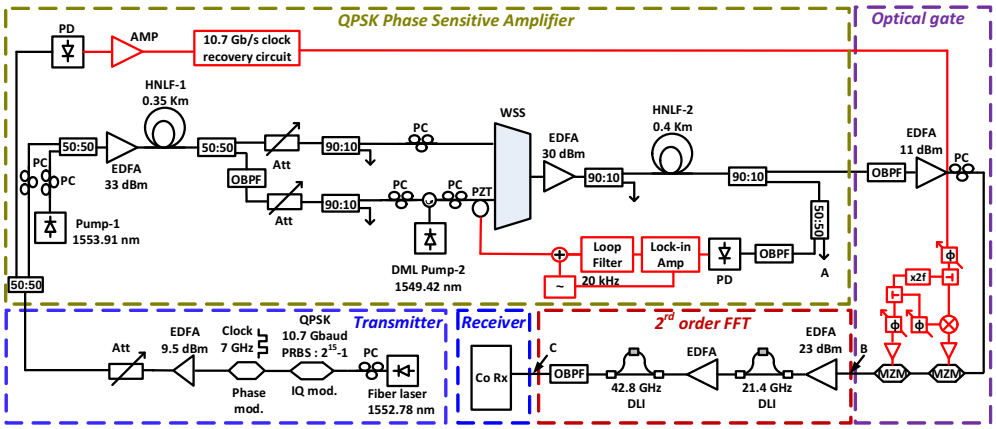

Fig. 4. Experimental setup of proposed PSA-based QPSK 3R regenerator.

two electro-optic Mach-Zehnder modulators (MZMs). The fist MZM was driven by a strong 21.4 GHz RF signal, which was obtained from the 10.7 GHz recovered clock and a frequency doubler, and it was biased at quadrature to produce a narrow pulse train. The second MZM suppressed every second pulse. To maximize this suppression, the drive signal for the second MZM was obtained by mixing the 21.4 GHz signal with the original 10.7 GHz RF and by aligning the time position of the resultant electrical pulse. This divided the sampling frequency by a factor of two and enabled a final switching window of reduced duration, i.e.12 ps, and of high contrast ratio, i.e. 35 dB. Optical gating is of course accompanied by spectral broadening, which reduces the compatibility of the system with high spectral efficient WDM systems. Thus the optical gate was followed by a spectral reshaping stage using an optical fast Fourier transform (FFT) [24], implemented using a cascade of two delay line interferometers (DLIs), of free spectral range 21.4 GHz and 42.8 GHz respectively, and a 0.4 nm optical band-pass filter (OBPF). This section of the system restores the NRZ pulse shape.

Finally, the signal was detected at the coherent receiver where it was sampled and digitized using a 80 GS/s real time oscilloscope with a 36 GHz analogue bandwidth. Channel estimation was performed off-line using conventional custom developed digital signal processing (DSP) algorithms for clock recovery and phase estimation [25].

4. Results and discussions

Each part of the 3R regenerator had been rigorously optimized to maximize the overall performance. At the synchronization stage a critical parameter to be fine tuned was the power ratio between the local Pump-1 and the incoming QPSK signal that were combined in the HNLF-1. In our case, the optimum point was when the cw pump power was 2.1 dB higher then the QPSK signal power, measured at the output of the HNLF-1. A higher power difference would decrease the strength of their FWM interaction, and consequently, the optical signal to noise ratio (OSNR) of the generated higher order harmonics. On the other hand, a reduced power difference would impose strong distortions due to self phase modulation effects. Similar optimizations have occurred at the regeneration stage of the PSA. At the WSS output, the power ratio of the QPSK signal to the 3rd harmonic was set at 8.9 dB to enable maximum suppression of the phase noise as predicted in [7]. In addition, the optimum power ratio of the two synchronized pumps to the QPSK signal was identified at 4.3 dB to avoid operation in the saturation regime that would otherwise increase non-linear distortion. Figure 5(a) shows two optical spec-

Optics EXPRESS

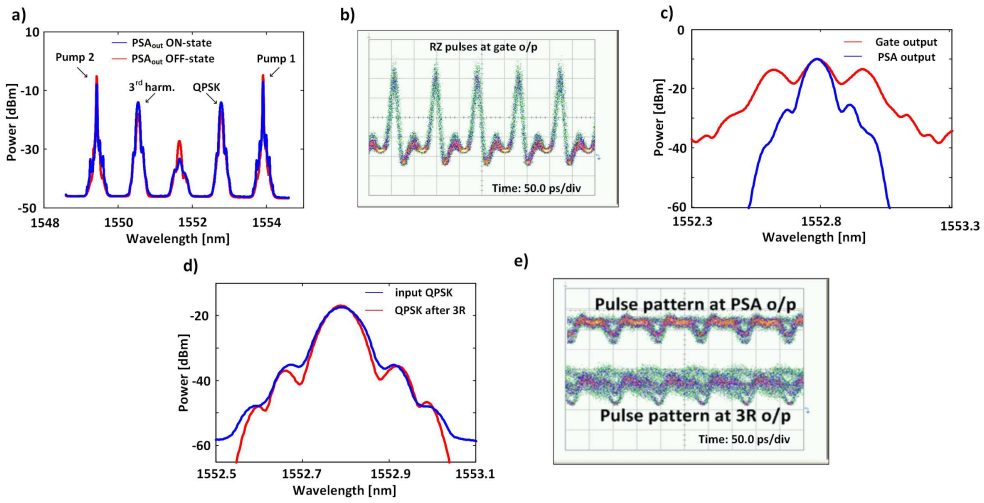

Fig. 5. (a) Optical spectrum at the output of the PSA for both maximum (ON, blue line) and minimum (OFF, red line) phase sensitive gain states (point-A). (b) RZ pulses at the output of the gate (point-B). (c) Optical spectra of the QPSK signal at the outputs of the gate (point-B, broadened) and the PSA (point-A). (d) Optical spectrum of the regenerated and retimed QPSK signal before coherent detection (point-C) overlapped with the input signal for comparison. (e) Pulse patterns at the output of the PSA (point-A) and the 3R (point-C).

tra at the output of the PSA (i.e. output of the HNLF-2), that corresponded to the cases where the amplifier has been locked in the maximum (i.e. ON) or in the minimum (i.e. OFF) phase sensitive gain state, respectively. The presence of this phase sensitive performance confirmed a working PSA, despite the fact that the measured power contrast ratio of the signal was significantly smaller (~ 3.5 dB) than a PSA operating case with BPSK signals (>10 dB). This is expected since the phase sensitive interaction occurs between waves of unequal amplitude. The waveform of the RZ-QPSK signal at the output of the optical gate is depicted in Fig. 5(b). The observed non-symmetry in the shape of the pulses is attributed to the limited spectral response of the oscilloscope used. The exact characteristics of the pulses were more accurately determined using a sub-picosecond time-scan method [16], which showed that a symmetric shape, 12 ps duration at full width at half maximum, and a contrast ratio of 35 dB are feasible. The depicted pattern in Fig. 5(b) corresponded to a gating configuration that enabled the best pulse reshaping and regeneration result. The sampling window was much shorter than the eye width and coincided with the center of the bit period, enabling the gate to suppress any pulse time jitter that may be developed during transmission or the regeneration process itself. The optical spectra at the PSA output and the output of the gate is shown in Fig. 5(c), showing the expected spectral broadening associated with optical sampling. The broadened spectrum was reshaped by the FFT filter recovering the spectrum of the original QPSK signal. This is clearly shown in Fig. 5(d) where the two spectra are compared. Finally, the recovered pattern after the pulse reshaping along with the pulse pattern at the output of the PSA are shown in Fig. 5(e). The broader pulse transitions were due to the non-ideal FFT response, approximated by the two cascaded DIs and the Gaussian bandpass filter. Improved pulse shapes can be expected when a more accurate FFT process is developed, i.e. either by increasing the number of cascaded DIs [24] or by using high resolution spectral processors [26].

The performance of the implemented regenerator was evaluated by measuring the Q^2-factor,

Optics EXPRESS

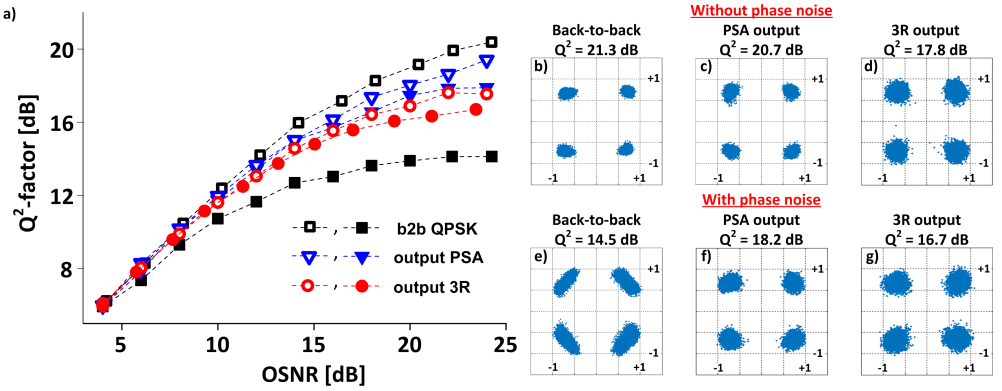

Fig. 6. (a) Q^2-factor measured at the input of the 3R regenerator and the outputs of the PSA stage and the retiming stage as a function of the OSNR degradation at the receiver: open symbols represent system performance without input phase noise and solid symbols with phase noise. Constellation diagrams of received signal: (b) at the input, (c) at the PSA (2R) output and (d) at the 3R output without input phase distortion, respectively; (e) at the input, (f) at the PSA (2R) output and (g) at the 3R output with input phase distortion.

calculated from the error vector magnitude (EVM) i.e. $Q^2[\text{dB}] = 10\log_{10}(1/\text{EVM}^2)$ [27] as a function of the optical signal-to-noise ratio (OSNR) for back-to-back transmission and transmission through the PSA stage and the retiming for two scenarios: i) when the input signal is free of phase noise, and ii) when it is heavily distorted in phase by introducing a 7 GHz tone to the phase modulator. The corresponding results are shown in Fig. 6(a). In the first case, and for an OSNR of 24 dB, the observed penalty between back-to-back and 3R output was less than 3.5 dB and it was mainly attributed to the non-ideally implemented FFT filter that was used for reshaping the pulses at the retiming section of the regenerator. When the signal was subjected to significant phase distortion, so that the input Q^2-factor was degraded to 14.5 dB, the 3R regenerator enabled a significant Q^2-factor improvement of 2.2 dB. The corresponding constellations of the aforementioned scenarios are depicted in Figs. 6(b)-6(g). Without distortion, a satisfying signal quality can be maintained at the 3R regenerator output with a Q^2-factor approaching 18 dB. For a degraded input, suppression of a significant amount of phase distortion (i.e. $\sim$ 40 degrees) is apparent with a Q^2-factor for the 3R regenerated constellation of 16.7 dB. Although the quality of the retimed and reshaped signal of Fig. 6(g) appears satisfactory, a small penalty is evident in the form of additional noise when compared to Fig. 6(f). This could be attributed to noise sampling by the optical gate and/or to intersymbol interference (ISI) resulting from non-ideal filtering. The spectral match can be improved by implementing a higher order FFT [24] and a more precise bias voltage control in the DLIs to take into account the finite width of the gating window (convolved with the impulse response of the filter) and the MZMs of the gate to optimise the window shape. Each Q^2-factor measurement in Figs. 6(a)-6(g) was obtained after processing $\sim$1.6M symbols. The averaging window of the Viterbi & Viterbi phase recovery algorithm was kept fixed to 7 bits.

5. Conclusion

We have presented, to the best of our knowledge, the first all-optical PSA-based 3R-regenerator for NRZ-QPSK modulated signals. The scheme combines the PSA element, which enables suppression of the phase noise, with an optical gate and a pulse reformatting filter for facilitating sampling at the minimum distortion point and the recovery of the NRZ signal at the output.

Optics EXPRESS

Through numerical simulations we have proved the 3R functionality of the scheme and its capability to improve significantly the transmission link performance. The experimental demonstration has shown more than 2.2 dB improvement in the Q^2-factor performance of the QPSK modulated data. The proposed solution can be made scalable to higher baud rates, thus enabling further enhancements in spectral efficiency.

Acknowledgments

This work has been supported by the Marie Curie - IEF project ARTISTE (IEF 330697), the EPSRC projects UNLOC and PEACE (EP/J017582/1 and EP/L000091/1) and the EU-ICT project FOX-C (grant number 318415). Finisar is acknowledged for providing the waveshaper for this experiment. Also, Dr Mary McCarthy is acknowledged for assistance with the transmitter configuration.